



Advancements in Lossless and Reversible Compression of Digital Pathology Images via Auto-Recursive Set Partitioning in Hierarchical Trees and Wavelet Decomposition

Goh Jee Yuan¹, Afzan Adam^{1*}, Mohammad Kamrul Hasan¹, Zaid Abdi Alkareem Alyasseri^{2,3},
Mohammad Faizal Ahmad Fauzi⁴, Elaine Wan Ling Chan⁵

¹ Center for Artificial Intelligence Technology, Faculty of Information Science and Technology, Universiti Kebangsaan Malaysia, Bangi 43300, Malaysia

² Information Technology Research and Development Center, University of Kufa, Kufa, Iraq

³ College of Engineering, University of Warith Al-Anbiyaa, Karbala, Iraq

⁴ Faculty of Engineering, Multimedia University, Jalan Multimedia, Cyberjaya 63100, Selangor, Malaysia

⁵ The Institute for Research, Development and Innovation, International Medical University, Kuala Lumpur 57000, Malaysia

Corresponding Author Email: afzan@ukm.edu.my

Copyright: ©2023 IETA. This article is published by IETA and is licensed under the CC BY 4.0 license (<http://creativecommons.org/licenses/by/4.0/>).

<https://doi.org/10.18280/ts.400632>

ABSTRACT

Received: 13 April 2023
Revised: 26 September 2023
Accepted: 18 October 2023
Available online: 30 December 2023

Keywords:

image compression, Set Partitioning in Hierarchical Trees, digital pathology, high resolution image

Set Partitioning in Hierarchical Trees (SPIHT) represents a leading-edge algorithm in near-lossless image compression, leveraging the Discrete Wavelet Transform. However, its effectiveness diminishes when applied to high-resolution images such as Digital Pathology Images (DPIs). This research aims to enhance the SPIHT algorithm specifically for DPIs by investigating the impact of applying various wavelets in the wavelet decomposition process and the introduction of auto-recursion in the SPIHT algorithm. An extensive selection of wavelet types were tested within the wavelet decomposition process integral to the SPIHT algorithm. The ultimate goal was to identify the wavelet that yields the highest compression ratio and the one that maintains the highest data consistency. The proposed auto-recursion was also examined against the original n-recursive algorithm to discern differences in compression performance. The results indicated that the BIOR 5.5 wavelet is more apt for achieving a high compression ratio, while the BIOR 3.9 wavelet is more suitable for securing high compression quality in the compression of high-resolution DPIs. The newly introduced auto-recursion feature contributes significantly to optimizing the quality of the compressed image. Visual verification of the compressed image's quality, for any potential loss of detail, was carried out through expert validation in a clinical setting. This expert validation confirmed that the proposed algorithm can produce higher quality compressed images with negligible loss of quality. Thus, this research offers a partial solution to current challenges in digital pathology related to storage, transfer, and archiving of high-resolution DPIs, by providing a more effective compression algorithm.

1. INTRODUCTION

Introduced in 1999, Virtual Slides (VS) represent a significant advancement in digital pathology, offering high-resolution images that permit microscope-like operations, such as panning, zooming, and navigating the image via a mouse and monitor [1]. Whether delineating a specific region or encompassing the entirety of a pathology slide, VS has begun to reshape the landscape of pathology diagnostics. Over a century of reliance on analog methods is gradually yielding to an era where examination of tissue and cell structures no longer necessitates physical contact with glass slides [2].

Prior to the advent of Whole Slide Imaging (WSI), the focus of pathologists was on static images, captured using microscope-specific optical cameras. These images allowed pathologists to highlight regions of interest from the whole slide for discussion and educational purposes. In contrast, WSI scanners capture sequential images in a tiled or line-scanning approach. These images are subsequently assembled or

stitched together to produce a VS, an exact digital replica of the glass slide [3].

The creation of such high-quality images involves several backend processes, including image acquisition, compression, storage, and visualization. A key determinant of the resolution of these digital images is the volume of data they contain. A large data volume typically yields an image of substantial size characterized by high resolution and distinct edges and features, culminating in a clear, crisp image [4-7]. Additionally, the quality of these medical images is heavily reliant on the level of noise and intensity in the image [8-10].

The essence of VS resides in its capacity to preserve the most minute details in the slides, a critical requirement for accurate diagnosis at the cellular and molecular level [11-14]. This necessity, however, leads to an increase in image size, making storage, transfer, and archiving tasks challenging [12, 15]. Consequently, image compression has been explored as a potential solution. By compressing the images, not only is transfer facilitated, but storage is also made more manageable

[16, 17].

The current standard compression in WSI is the JPEG2000 compression scheme, which is based on discrete wavelet transform [12]. While it has been reported as a useful tool for image compression, it falls short of meeting the contemporary image advancement criteria [18]. Despite several enhancements to the JPEG2000 algorithm aimed at further lossless compression, the effectiveness of these improvements is contingent on the image type [19, 20]. Some providers of virtual slide imaging systems have resorted to proprietary file formats specifically designed for storing high-resolution slide images. These formats often incorporate custom-made compression algorithms tailored to their specific systems. The stark differences in the magnification of VS are evident in Figure 1.

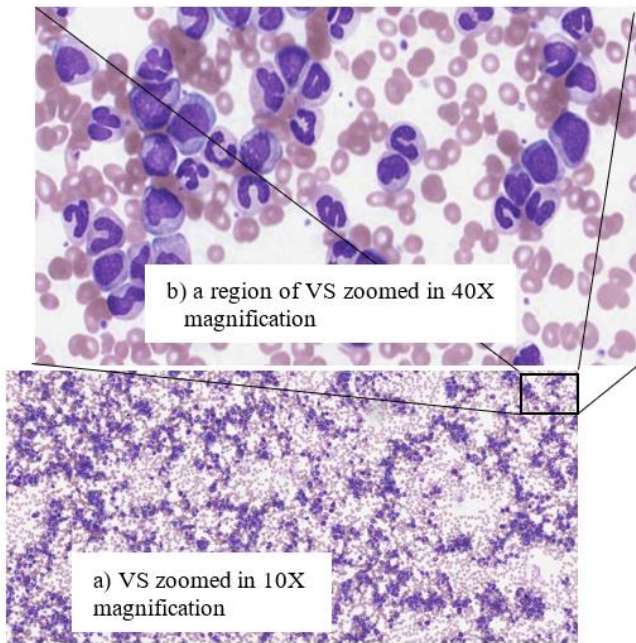


Figure 1. a) VS (blood smear) zoomed at 10X with 6761*3876 pixels, and b) zoomed 40X with dimensions of 2000*1691 pixels

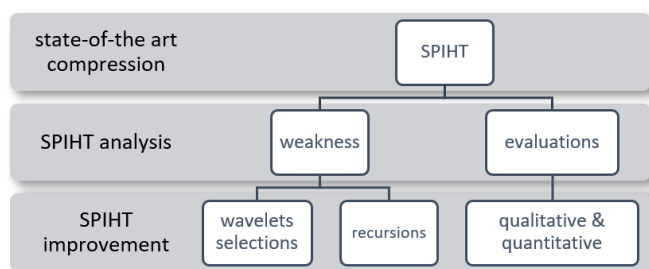


Figure 2. Structure of paper

On the contrary, the Set Partitioning in Hierarchical Trees (SPIHT) image compression algorithm currently represents the state-of-the-art in wavelet-based image compression. Notably, the SPIHT compression algorithm is renowned for its ability to produce high-quality compressed images and has recently gained traction in the compression of MRI images [21].

However, the SPIHT compression algorithm has yet to be tested on high-resolution images, particularly Virtual Slides (VS). Furthermore, the current implementations of the SPIHT algorithm are less autonomous, requiring users to input specific parameters. The algorithm then operates recursively based on these set parameters. Conversely, the JPEG2000 compression algorithm follows a fixed format, necessitating users to possess specific software to view, edit, or utilize images in the JPEG2000 format. Therefore, the focus of this paper lies in the analysis of the SPIHT algorithm, exploration of methods to enhance SPIHT, particularly with respect to the compression of high-resolution VS, and presentation of the evaluation results of these improvements.

The structure of this paper is depicted in Figure 2. It commences with a discussion on the current work involving SPIHT and an analysis of the SPIHT algorithm, followed by the presentation of the acquired results.

2. BACKGROUND STUDY

Numerous image compression algorithms have been investigated for their potential in compressing medical images, including the Set Partitioning in Hierarchical Trees (SPIHT) algorithm. In 2020, Miya proposed a SPIHT image compression algorithm specifically designed for compressing medical images. The research outlined two wavelet variations: the HAAR wavelet and the Biorthogonal 4.4 wavelet. Recursion was also tested in the study, although it primarily focused on MRI images of kidneys. The recursion aspect of the algorithm was examined by manually adjusting the recursion limiter number (N) in each iteration, but this was only tested within a range from n=0 to n=15 [22].

In a similar vein, Sran proposed a SPIHT image compression algorithm for compressing brain MRI images, introducing a novel function that separates a Region-of-Interest (ROI) from the images. This ROI is compressed at high quality, while the remainder of the image, deemed of lesser importance, is compressed at lower quality to achieve higher compression rates [23]. However, this strategy of reducing complexity by selecting specific features for compression is not particularly effective when applied to Virtual Slides (VS), where every segment of the image holds significance for pathologists during diagnosis. Moreover, when the entirety of the image is selected as the ROI, the compression quality is poorer compared to the application of the original SPIHT image compression algorithm on the whole image.

In 2021, Ahmed proposed a SPIHT image compression algorithm for compressing MRI images. This research emphasized a hybridized transform technique, whereby the curvelet transform supersedes the wavelet transform when processing the LH, HL, HH bands in forward and inverse transform procedures. This hybridized transform enables more detailed control as it further decomposes the bands into three layers: coarse, detail, and fine layers for processing [24-28]. However, this approach increases the algorithm's complexity, leading to higher computational costs. Table 1 provides a summary of previous work conducted in the field of SPIHT.

Table 1. Previous works in SPIHT

Author	Variation	Method	Modality	Gap
Miya, 2020	Wavelet	HAAR	Kidney MRI	1. Recursions beyond n=15 not tested. 2. Only tested on kidney MRI images.
	Wavelet Recursion	BIOR 4.4 n=0 to n=15		
Sran, 2020	Wavelet Zone	DB 4 Region-of-interest	Brain MRI	1. Lower performance than original when compressing whole image. 2. Only tested on brain MRI images.
Ahmed, 2021	Wavelet	Hybridization	MRI Images	1. Small sample size of only four images.

3. METHODOLOGY

3.1 Material

The data used for this research are 50 pathology slide scans that are ethically obtained from Hospital Canselor Tuanku Muhriz UKM (HCTM) with the help of pathologists (JEP-2020-134). The slides are then converted to high-resolution digital pathology slides using a slide scanner. The digital slides have an average dimension of 100,000 pixels in width and 80,000 pixels in height, with an average uncompressed file size of 30 gigabytes each.

In the pre-processing phase, the individual digital slides are then split into multiple tiles for ease of processing as the slides are too big to be processed as a whole. Each tile measures 2048 pixels in width and height respectively. Each digital slide is split into 2000 tiles on average, which then forms the dataset for the research. Figure 3 shows two sample images from HUKM_DP the dataset.

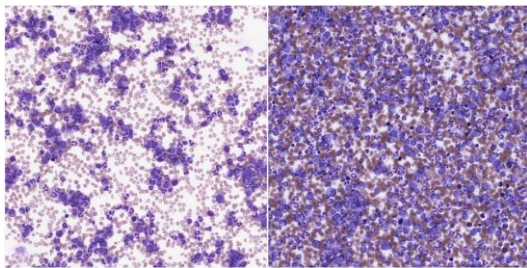


Figure 3. Sample image from HUKM_DP dataset

3.2 SPHIT analysis

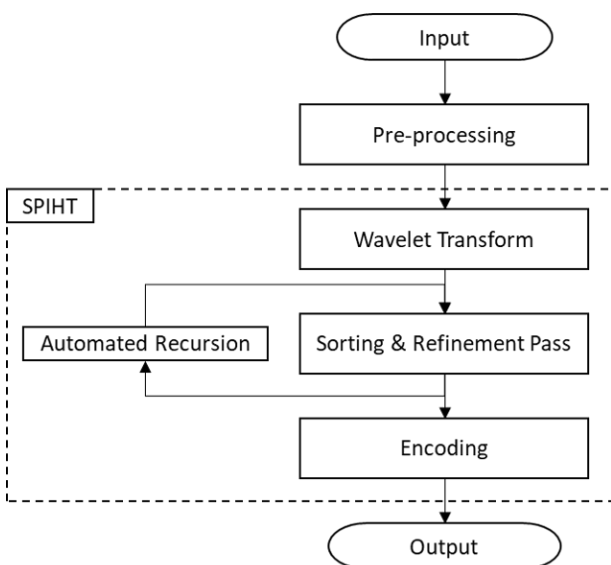


Figure 4. Block diagram for compression procedure

The block diagram for this research is presented in Figure 4 below. The research is carried out in sequence as follows: Pre-processing, Wavelet Transform, Sorting & Refinement Pass, and Automated Recursion.

In the wavelet transform phase, the dataset is fed through the SPIHT image compression algorithm. However, which wavelet variation within SPIHT would be the best fit for the compression of high-resolution digital pathology images are not known. Thus, a wavelet has to be selected as the base wavelet for decomposition. Common wavelet options that are selected for wavelet decomposition are usually from the Haar and Daubechies(db) wavelet families (25) as they have been extensively used by numerous researchers since the early days of SPIHT and still remains a popular option even till this very day. In this research however, a few other wavelet families are tested on top of those two, to discover which wavelet and its variation works best when compressing high-resolution digital pathology images.

The wavelet families that are tested in this research are as follows: Biorthogonal wavelets, Coiflets, Daubechies wavelets, Discrete Meyer wavelet, Fejér-Korovkin filters, Haar wavelet, Reverse biorthogonal wavelets and Symlets. However, there could be more wavelets that are available which are not tested in this research which may give different results. Table 2 shows the list of wavelet families and its variations which will be tested in this research. Once all wavelets are tested, the results are recorded for further analysis in the result analysis phase.

Table 2. List of tested wavelets

Wavelet	Variations
Discrete Meyer	DMEY
Haar	HAAR
Fejér-Korovkin	FK4, FK6, FK8, FK14, FK18, FK22
Coiflet	COIF1, COIF2, COIF3, COIF4, COIF5
Symlet	SYM2, SYM3, SYM4, SYM5, SYM6, SYM7, SYM8
Daubechies	DB1, DB2, DB3, DB4, DB5, DB6, DB7, DB8, DB9, DB10
Reverse Biorthogonal	RBIO1.1, RBIO1.3, RBIO1.5, RBIO2.2, RBIO2.8, RBIO3.7, RBIO3.9, RBIO4.4, RBIO5.5, RBIO6.8
Biorthogonal	BIOR1.1, BIOR1.3, BIOR1.5, BIOR2.2, BIOR2.4, BIOR2.6, BIOR2.8, BIOR3.1, BIOR3.3, BIOR3.5, BIOR3.7, BIOR3.9, BIOR4.4, BIOR5.5, BIOR6.8

3.3 SPHIT improvement

In this phase, the recursion module in the SPIHT algorithm, which allows the wavelet decomposition process to recursively call upon itself, is automated through this research. Instead of the usual, where the maximum amount of recursion

passes is defined by the user beforehand, the recursion process is instead automated, where the process automatically recurses to the point where any further recursion would not bring any improvement and would be redundant, in order to bring out the maximum performance of the compression algorithm in terms of image quality.

Figure 5 shows the proposed automated recursion module. Once the data passes through the wavelet transform procedure,

the List of Insignificant Pixels (LIP), List of Insignificant Sets (LIS), and List of Significant Pixels (LSP) are generated. The data is then sorted into those lists based on the algorithm's threshold levels, and the data in the list is then parsed accordingly. Once the data has been parsed, if there is any change to the data, it is then re-sorted into their respective lists based on the threshold. The automated recursion module then checks for the number of recursions.

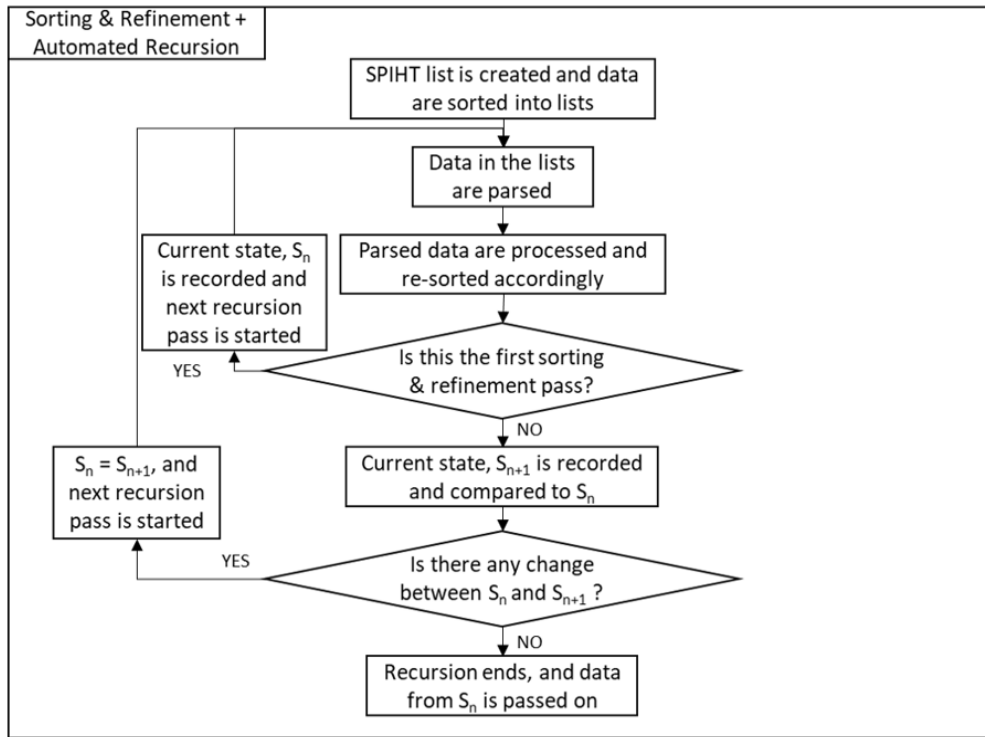


Figure 5. Proposed automated recursion module

If this is the first pass, where the number of recursions, n is 0, then the current state is recorded as S_0 and the next recursion call is automatically started, where the data in the re-sorted lists are then parsed again, and re-sorted accordingly, if any data passes the set threshold again after the first recursive pass.

From the second pass onwards, the current state of the data is recorded as S_{n+1} and is compared with against S_n . If there is any change or difference between the states S_{n+1} and S_n , it marks that there has been an improvement to the data, hence the S_{n+1} state overrides the S_n state and the next recursive pass is called. This happens until a situation where there is no change between the states S_{n+1} and S_n , which marks that the data can no longer be improved by recursive passes, and any recursion from this point onwards will only be redundant. The automated recursion module then ends, and the data from the S_n state is passed on for encoding. By adding a stopping criterion to the loop, the best case scenario for this improved SPHIT can be $\Omega(n)$ as recursive might not be needed anymore.

The compression performance of the algorithm with the automated recursion module is then tested by running the compression once again on the same dataset. The results are recorded for further analysis.

Once the compression process is completed and the reconstructed images are obtained, the compression quality is then evaluated by measuring CR and PSNR values of each compression. By evaluating these parameters, a quantifiable measure of the quality of the compression, in terms of both

compression strength and image quality, can be obtained. The best wavelet for compression strength and image quality respectively can then be found. Also, a comparison between the compression performance of the automated and non-automated recursion module can be measured.

3.4 Evaluation parameters

The performance of an image compression algorithm can be evaluated through different aspects, whether it be in terms of how much compression has been done, or in terms of the quality of the compressed image [26].

In order to measure the amount of compression that had been applied, Compression Ratio (CR) is used. CR refers to the ratio between the number of bits in the original image against the number of bits in the compressed image, where a higher CR means that the file has been highly compressed. The equation to determine CR is as follows:

$$CR = \frac{\text{Number of Bits in Original Image}}{\text{Number of Bits in Compressed Image}} \quad (1)$$

In order to measure the quality of the compressed image, Peak Signal-to-Noise Ratio (PSNR) is used. PSNR is measure in decibels (dB), and represents the clarity or quality of the images in relevance to the size of the error, where a high PSNR value represents a low size of error in the compressed image, or a high-quality compressed image is produced. The equation

to determine PSNR is as follows:

$$PSNR = 10 \log_{10} \frac{((2^b)-1)^2}{MSE} \quad (2)$$

$$MSE = \frac{1}{mn} \sum_{i=0}^{m-1} \sum_{j=0}^{n-1} (Y_{i,j} - \hat{Y}_{i,j})^2 \quad (3)$$

where, b is the maximum number of bits per pixel, m and n are the maximum width and height of the image respectively, Y is a pixel on the original image with coordinates (i,j) , and \hat{Y} is a pixel on the compressed image with coordinates (i,j) .

3.5 Clinical evaluation

In order to visually verify the results of the compression, twenty pathologists were selected at random from HCTM to serve as domains experts for visual verification of the quality of the images. These expert domains are required to seat for an online survey which contains 2 sections.

The first section contains fifteen pair of images. The respondents were asked to select the clearer image between two similar images, where the images presented were between the ones produced by the proposed algorithm against the SPIHT algorithm.

In the second section, which also consists of another fifteen pair of images, the respondents were asked if there were any discernible loss of detail between the two presented images which would affect their diagnosis, where the images are between the ones produced by the proposed algorithm against the original image.

All images used in the questionnaire are selected randomly, placed in random order, and displayed with the same display device. The respondents were not given any info prior to answering the questionnaire.

The questionnaire serves to verify if whether the pathologists can indeed visually observe the quality improvement between the images produced by the proposed algorithm against the SPIHT algorithm, and also to verify that there is no loss of detail between the images produced by the proposed algorithm against the original image.

3.6 Clinical evaluations

In order to visually verify the results of the compression, twenty pathologists were selected at random from HCTM to serve as domains experts for visual verification of the quality of the images. These expert domains are required to seat for an online survey which contains 2 sections.

The first section contains fifteen pair of images. The respondents were asked to select the clearer image between two similar images, where the images presented were between the ones produced by the proposed algorithm against the SPIHT algorithm.

In the second section, which also consists of another fifteen pair of images, the respondents were asked if there were any discernible loss of detail between the two presented images which would affect their diagnosis, where the images are between the ones produced by the proposed algorithm against the original image.

All images used in the questionnaire are selected randomly, placed in random order, and displayed with the same display device. The respondents were not given any info prior to answering the questionnaire.

The questionnaire serves to verify if whether the

pathologists can indeed visually observe the quality improvement between the images produced by the proposed algorithm against the SPIHT algorithm, and also to verify that there is no loss of detail between the images produced by the proposed algorithm against the original image.

4. RESULT AND DISCUSSION

Table 3. Results of testing varying wavelets with SPIHT

Wavelet	CR	PSNR (dB)	SSIM (%)
BIOR 1.1	29.4321	41.1022	97.6950
BIOR 1.3	25.7942	41.5721	97.8183
BIOR 1.5	24.6567	41.0681	97.7154
BIOR 2.2	34.7661	42.7298	98.2409
BIOR 2.4	32.9719	43.0507	98.3232
BIOR 2.6	31.8715	43.1721	98.3545
BIOR 2.8	31.1469	43.2107	98.3625
BIOR 3.1	49.5145	40.2996	97.3876
BIOR 3.3	23.3788	43.3476	98.4346
BIOR 3.5	23.6553	43.6104	98.4936
BIOR 3.7	23.5376	43.6207	98.5042
BIOR 3.9	23.3891	43.7261	98.5243
BIOR 4.4	52.6860	42.1882	98.0449
BIOR 5.5	73.7624	41.1724	97.6855
BIOR 6.8	47.3526	42.6066	98.1645
COIF 1	40.4681	42.0384	97.9884
COIF 2	46.4208	42.4226	98.1033
COIF 3	47.8477	42.4573	98.1088
COIF 4	48.2989	42.4808	98.1202
COIF 5	48.5765	42.5224	98.1329
SYM 2	39.8918	41.9565	97.9786
SYM 3	44.1829	42.3079	98.0662
SYM 4	45.8175	42.4016	98.0966
SYM 5	47.3930	42.4349	98.1044
SYM 6	47.3407	42.4890	98.1210
SYM 7	47.9478	42.4884	98.1224
SYM 8	47.9231	42.4951	98.1281
DB 1	29.4324	41.1022	97.6950
DB 2	39.8920	41.9565	97.9786
DB 3	44.1832	42.3079	98.0662
DB 4	46.0598	42.3743	98.0924
DB 5	46.7464	42.4379	98.1090
DB 6	47.0461	42.4470	98.1121
DB 7	47.5340	42.4781	98.1246
DB 8	47.2501	42.4723	98.1250
DB 9	47.5171	42.5032	98.1303
DB 10	47.7667	42.4836	98.1302
DMEY	48.8093	42.5738	98.1483
FK 4	32.7378	41.6448	97.8743
FK 6	44.2695	42.2537	98.0608
FK 8	46.4408	42.4368	98.1062
FK 14	47.7794	42.4946	98.1346
FK 18	48.2690	42.5497	98.1474
FK 22	47.8814	42.5448	98.1462
HAAR	29.4323	41.1022	97.6950
RBIO 1.1	29.4321	41.1022	97.6950
RBIO 1.3	51.0666	41.8967	97.9456
RBIO 1.5	54.8524	41.9222	97.9562
RBIO 2.2	34.1890	40.0716	97.1192
RBIO 3.9	57.8563	41.3367	97.7116
RBIO 4.4	49.0508	38.9710	96.4904
RBIO 5.5	52.5052	39.2638	96.6756
RBIO 6.8	37.9748	42.4642	98.1053

The findings of this research were recorded and the results of the performance of the tested wavelets were tabulated. Table 3 shows the compression performance of each wavelet tested. It also shows that each wavelet produces a different

result for the compression of the high-resolution digital pathology images. Thus, we can say that the wavelet used does indeed affect the results of the compression. The table can then be summarized to show the best performing wavelet in terms of compression, measured by CR; while image quality was measured by PSNR from each wavelet family.

Figure 6 shows the best performing wavelet in each category from each wavelet family. Figure 6 shows that the wavelet which produces the highest compression is the BIOR 5.5 wavelet, with a CR of 73.7624, while the wavelet which produces the image with the highest quality is the BIOR 3.9 wavelet, with a PSNR of 43.7261dB.

Table 4 shows the compression performance between the non-automated recursion SPIHT algorithm against the automated recursion SPIHT algorithm, where both algorithms applied the BIOR 3.9 wavelet.

Table 4 also shows that while the automated recursion method produces a higher compressed image quality, it is achieved at the cost of compression power when compared to the non-automated recursion method, as seen by the CR value of 10.1413 of the automated recursion methods, against 23.3891 of the non-automated recursion methods. Also, we can say that the automated recursion method does produce a higher compressed image quality, as seen by the PSNR value of 51.5543dB, when compared to the non-automated recursion method, with PSNR value of 43.7261dB.

From the results, the SPIHT image compression technique which utilizes the BIOR 5.5 wavelet produces the highest compression when compressing high-resolution digital pathology images, while the BIOR 3.9 wavelet produces the best quality when compressing high-resolution digital pathology images. This indicates that the BIOR wavelet family is a good wavelet choice for image compression involving wavelet transforms.

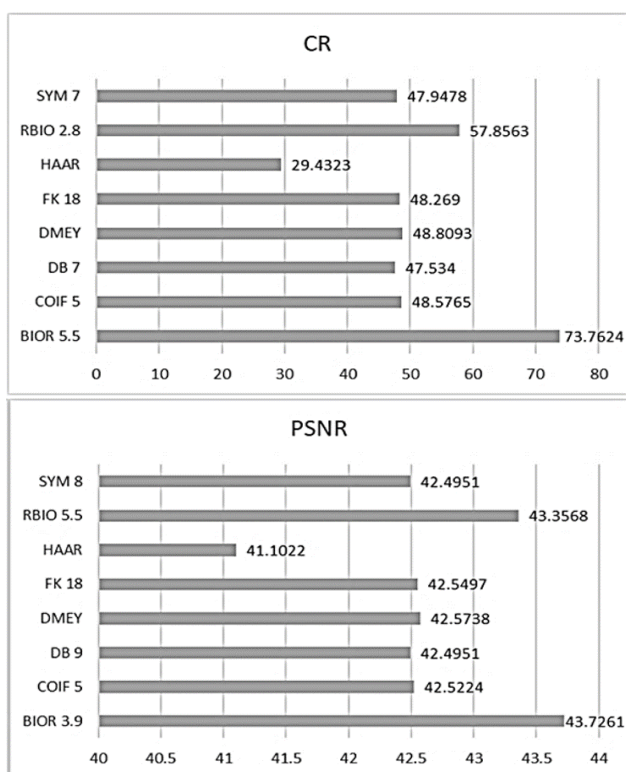


Figure 6. Best performing wavelet in terms of CR and PSNR from each wavelet family

Table 4. Result of original recursion against the automated recursion

Method	CR	PSNR (dB)	SSIM (%)
original Recursion	23.3891	43.7261	98.5243
Automated Recursion	10.1413	51.5543	99.8390

It is also worth noted that the automated recursion module produces a better result than the manual recursion method, with a PSNR of 51.5543dB against 43.7261dB. This is most probably due to the quality optimization done by the automated recursion module, where it automatically finds the highest level of recursion that can be done to the image before it reaches redundancy, as compared to a predetermined level of recursion by the user in the manual recursion method, where the user has no idea whether if the determined level of recursion is sufficient, or the best, or redundant.

Table 5 shows the results of the clinical setup evaluation. Where the scores for section 1 shows the mean score of respondents selecting the image produced by the proposed algorithm as the sharper image against the image produced by SPIHT, and the scores for section 2 shows the mean percentage of respondents that decided that there would be no difference between the image produced by the proposed algorithm against the original image.

Table 5 shows that in general, the respondents were able to select the image produced by proposed algorithm as the sharper image when compared against the image produced by the SPIHT algorithm, resulting in an average accuracy score of 86.67%. This has proved that the proposed algorithm has produced better image than current compression algorithm. The only 4 images with scores lower than 75.00% were images 4, 6, 11, and 12. From the feedback received by the respondents, this is due to bad sampling of the original image, where a bad scanning technique of the original image caused a low-quality original image, which in turns affects the quality of the compressed images where both the image produced by the proposed algorithm and the SPIHT algorithm are low in quality.

Table 5 also shows that for section 2 in general, the respondents had decided that there would not be any discernible loss of details between the image produced by the proposed algorithm against the original image, as seen by the average score of 99.00% where only 1 respondent had a different opinion for images 8, 11, and 13.

Hence, we can say that by changing the wavelet used in the SPIHT algorithm, we have achieved a better result in terms of compressed image quality when compared to previous studies. Furthermore, the quality of the compressed image is further optimized through the use of the automated recursion algorithm, instead of ending abruptly due to manual recursion. The clinical evaluation has also proven that the image produced by the proposed algorithm is indeed sharper than that produced by the SPIHT algorithm; and does not suffer from any visually discernible detail loss when compared to the original image.

Table 5. Results for clinical setup evaluation

Section	Average Score	ID with < Average Score
1 (if proposed algorithm produced better image)	85%	4,6,11,12
2 (if produced image had retain the image's details)	99%	8,11,13

5. CONCLUSION

This paper investigates the quality of the compressed image by the SPIHT algorithm in the compression of high-resolution digital pathology images. Through changing of wavelet and automating the recursion module, it has been proven that this is a viable solution to solve storage and transfer issues. This paper proposed a modified SPIHT algorithm that suited for compression of high resolution digital pathology images. An automated recursion SPIHT algorithm was enhanced with the BIOR 3.9 wavelet, and auto-recursion module for the functionality of producing the highest image quality and optimize quality of the compressed image.

The experimental results of this research conclude that the modification has indeed produced a better result in the compression of high-resolution digital pathology images and is indeed a viable solution to storage issues. The automated recursion module is indeed able to display the compressed image with a higher image quality, with a PSNR value of 51.5543dB as compared to 43.7261dB when using the original SPHIT recursion option. On top of this, 99% agreement during clinical verification which were carried out as double blind review process and standardized display device for all evaluators.

The proposed algorithm managed to better compress the digital pathology images, which were way higher resolution compared to radiology images. Thus, it shouldn't have any problem to compress a lower resolution image.

However, there were limitations in which this paper lacked in. One such was that the algorithm was not optimized in terms of complexity as the focus of the paper was on maximizing image quality. Another limitation would be that as the algorithm was tested on high-resolution digital pathology images only and not on other commonly tested images such as CT, X-ray and MRI, hence we cannot claim that this would be the best algorithm for all types of medical images. There is however, much potential for future research in terms of optimizing the complexity of the algorithm for a faster algorithm, or perhaps in the direction of a new wavelet which would produce a compression with a higher image quality or in the direction of improving compression rates while maintaining the current image quality.

ACKNOWLEDGEMENTS

The authors would like to acknowledge Medical Computing Group, the Center of Research and Instrumentation Management (CRIM), Universiti Kebangsaan Malaysia and the Ministry of Higher Education, Malaysia for supporting the research with funding through project code: [KKP/2020/MMU-UKM/7/2]. This research and data usage are approved by the Universiti Kebangsaan Malaysia Hospital Research Ethics Secretariat (JEP-2020-134 & JEP-2022-317).

REFERENCES

- [1] Zarella, M.D., Bowman, D., Aeffner, F., Farahani, N., Xthona, A., Absar, S.F., Parwani, A., Bui, M., Hartman, D.J. (2019). A practical guide to whole slide imaging: A white paper from the digital pathology association. *Archives of Pathology & Laboratory Medicine*, 143(2): 222-234. <https://doi.org/10.5858/arpa.2018-0343-RA>
- [2] Nam, S., Chong, Y., Jung, C.K., Kwak, T.Y., Lee, J.Y., Park, J., Rho, M.J., Go, H. (2020). Introduction to digital pathology and computer-aided pathology. *Journal of Pathology and Translational Medicine*, 54(2): 125-134. <https://doi.org/10.4132/jptm.2019.12.31>
- [3] Godinho, T.M., Lebre, R., Silva, L.B., Costa, C. (2017). An efficient architecture to support digital pathology in standard medical imaging repositories. *Journal of Biomedical Informatics*, 71: 190-197. <https://doi.org/10.1016/j.jbi.2017.06.009>
- [4] Tyagi, V. (2018). *Understanding Digital Image Processing*. Understanding Digital Image Processing, CRC Press.
- [5] Adam, A., Rahman, A.H.A., Sani, N.S., Alyessari, Z.A.A., Mamat, N.J.Z., Hasan, B. (2021). Epithelial layer estimation using curvatures and textural features for dysplastic tissue detection. *CMC- Computers, Materials & Continua*, 67: 761-777. <http://dx.doi.org/10.32604/cmc.2021.014599>
- [6] Sahran, S., Qasem, A., Omar, K., Albashih, D., Adam, A., Abdullah, S.N.H.S., Abdullah, A., Hussain, R.I., Ismail, F., Abdullah, N., Pauzi, S.H.M., Abd Shukor, N. (2018). *Machine Learning Methods for Breast Cancer Diagnostic*. Breast Cancer and Surgery.
- [7] Daud, M.M., Zaki, W.M.D.W., Hussain, A., Mutalib, H.A. (2020). Keratoconus detection using the fusion features of anterior and lateral segment photographed images. *IEEE Access*, 8: 142282-142294. <https://doi.org/10.1109/ACCESS.2020.3012583>
- [8] Ibrahim, R.W., Jalab, H.A., Karim, F.K., Alabdulkreem, E., Ayub, M.N. (2022). A medical image enhancement based on generalized class of fractional partial differential equations. *Quantitative Imaging in Medicine and Surgery*, 12(1): 172-183. <https://doi.org/10.21037/qims-21-15>
- [9] Radhika, R., Mahajan, R. (2022). Medical Image Enhancement: A Review. In: Saraswat, M., Roy, S., Chowdhury, C., Gandomi, A.H. (eds) *Proceedings of International Conference on Data Science and Applications*. Lecture Notes in Networks and Systems, vol 288. Springer, Singapore. https://doi.org/10.1007/978-981-16-5120-5_9
- [10] Yousif, A.S., Sheikh, U.U., Omar, Z. (2019). A novel enhancement method for medical image using double density wavelet and stationary wavelet transforms. In *2019 IEEE 9th International Conference on System Engineering and Technology (ICSET)*, Shah Alam, Malaysia, pp. 292-297. <https://doi.org/10.1109/ICSEngT.2019.8906378>
- [11] Azam, A.S., Miligy, I.M., Kimani, P.K., Maqbool, H., Hewitt, K., Rajpoot, N.M., Snead, D.R. (2021). Diagnostic concordance and discordance in digital pathology: a systematic review and meta-analysis. *Journal of Clinical Pathology*, 74(7): 448-455. <http://dx.doi.org/10.1136/jclinpath-2020-206764>
- [12] Aeffner, F., Adissu, H. A., Boyle, M.C., Cardiff, R.D., Hagendorn, E., Hoenerhoff, M.J., Klopffleisch, R., Newbigging, S., Schaudien, D., Turner, O., Wilson, K. (2018). Digital microscopy, image analysis, and virtual slide repository. *ILAR Journal*, 59(1): 66-79. <https://doi.org/10.1093/ilar/ily007>
- [13] Adam, A., Bulpitt, A., Treanor, D. (2012). Grading dysplasia in Barrett's oesophagus virtual pathology slides with cluster co-occurrence matrices. In *Proc. of*

- Histopathology Image Analysis: Image Computing in Digital Pathology in conjunction with the 15th International Conference on Medical Image Computing and Computer Assisted Intervention (MICCAI).
- [14] Adam, A., Mudjahidin, A.A.I., Hasan, B., Albashish, D. (2020). Injecting tissue texture and morphology comprehension into algorithm for cancer grading. *Test Eng Manage*, 83: 17489-17497.
- [15] Lee, L.M., Goldman, H.M., Hortsch, M. (2018). The virtual microscopy database—sharing digital microscope images for research and education. *Anatomical Sciences Education*, 11(5): 510-515. <https://doi.org/10.1002/ase.1774>
- [16] Singh, S., Sood, V., Sharma, B. (2020). Systematic survey of compression algorithms in medical imaging. In *Advances in Computational Techniques for Biomedical Image Analysis*, pp. 205-230. Academic Press. <https://doi.org/10.1016/B978-0-12-820024-7.00011-6>
- [17] Hussain, A.J., Al-Fayadh, A., Radi, N. (2018). Image compression techniques: A survey in lossless and lossy algorithms. *Neurocomputing*, 300: 44-69. <https://doi.org/10.1016/j.neucom.2018.02.094>
- [18] Krishnan, S., Sathe, P.M. (2013). Comparison of IRIS image compression using JPEG 2000 and SPIHT algorithm. *IOSR Journal of Electronics and Communication Engineering*, 4(4): 5-9.
- [19] Du, Q., Fowler, J.E. (2007). Hyperspectral image compression using JPEG2000 and principal component analysis. *IEEE Geoscience and Remote Sensing Letters*, 4(2): 201-205. <https://doi.org/10.1109/LGRS.2006.888109>
- [20] Gungor, M.A., Gencol, K. (2020). Developing a compression procedure based on the wavelet denoising and JPEG2000 compression. *Optik*, 218: 164933. <https://doi.org/10.1016/j.ijleo.2020.164933>
- [21] Kalaiselvi, K. (2017). Image compression using SPIHT techniques. *Journal of Mathematics and Informatics*, 11: 147-153. <http://dx.doi.org/10.22457/jmi.v11a19>
- [22] Miya, J., Ansari, M.A. (2020). Medical images performance analysis and observations with SPIHT and wavelet techniques. *Journal of Information and Optimization Sciences*, 41(1): 273-282. <https://doi.org/10.1080/02522667.2020.1721616>
- [23] Sran, P.K., Gupta, S., Singh, S. (2020). Segmentation based image compression of brain magnetic resonance images using visual saliency. *Biomedical Signal Processing and Control*, 62: 102089. <https://doi.org/10.1016/j.bspc.2020.102089>
- [24] Ahmed, L.J., Fathima, B.A., Mahaboob, M., Gokulavasan, B. (2021). Biomedical image processing with improved SPIHT algorithm and optimized curvelet transform technique. In *2021 7th International Conference on Advanced Computing and Communication Systems (ICACCS)*, Coimbatore, India, pp. 1596-1602. <https://doi.org/10.1109/ICACCS51430.2021.9441832>
- [25] Ghazali, K.H., Mansor, M.F., Mustafa, M.M., Hussain, A. (2007). Feature extraction technique using discrete wavelet transform for image classification. In *2007 5th Student Conference on Research and Development*, Selangor, Malaysia, pp. 1-4. <https://doi.org/10.1109/SCORED.2007.4451366>
- [26] Hoshi, A.R., Zainal, N., Ismail, M., Rahem, A.A.R.T., Wadi, S.M. (2021). A robust watermark algorithm for copyright protection by using 5-level DWT and two logos. *Indonesian Journal of Electrical Engineering and Computer Science*, 22(2): 842-856. <https://doi.org/10.11591/ijeecs.v22.i2.pp842-856>
- [27] Varish, N., Pal, A.K., Hassan, R., Hasan, M.K., Khan, A., Parveen, N., Banerjee, D., Pellakuri, V., Ul Haqis, A., Memon, I. (2020). Image retrieval scheme using quantized bins of color image components and adaptive Tetrolet transform. *IEEE Access*, 8: 117639-117665. <https://doi.org/10.1109/ACCESS.2020.3003911>
- [28] Hasan, M.K., Ghazal, T.M., Alkhalifah, A., Abu Bakar, K.A., Omidvar, A., Nafi, N.S., Agbinya, J.I. (2021). Fischer linear discrimination and quadratic discrimination analysis-based data mining technique for internet of things framework for Healthcare. *Frontiers in Public Health*, 9: 737149. <https://doi.org/10.3389/fpubh.2021.737149>